~~On the periodicity~~ Thermodynamic evolution of ~~free oscillations for~~ a finite ice column: analytical solution and basal-melting timescales

Daniel Moreno-Parada[1,2], Alexander Robinson[1,2], Marisa Montoya[1,2], and Jorge Alvarez-Solas[1,2]

[1]Departamento de Física de la Tierra y Astrofísica, Universidad Complutense de Madrid, Facultad de Ciencias Físicas, 28040 Madrid, Spain

[2]Instituto de Geociencias, Consejo Superior de Investigaciones Científícas-Universidad Complutense de Madrid, 28040 Madrid, Spain

Correspondence: Daniel Moreno-Parada (danielm@ucm.es)

Abstract. The temperature distribution in ice sheets is worthy of attention given the strong relation with ice dynamics and the intrinsic information about past surface temperature variations. Here we refine the classical analysis of free oscillations in an ice sheet by analytically solving the thermal evolution of an ice column. In so doing, we provide analytical solutions to the one-dimensional Fourier heat equation over a finite motionless ice column for a ~~general~~ more general (Robin) boundary condition problem. The time evolution of the temperature profiles appears to be strongly dependent on the column thickness L and largely differs from previous studies that assumed an infinite column thickness. Consequently, the time required for the column base to thaw depends on several factors ~~: the ice column thickness L,~~ besides the ice thermal properties: the initial temperature profile~~and~~, the boundary conditions and the ice-column thickness L. This timescale is classically considered to be the period of a binge-purge oscillator, a potential mechanism behind the Heinrich Events. Our analytical solutions show a broad range of periods for ~~medium-size~~ typical-size column thicknesses. In the limit ~~of~~ $L \rightarrow \infty$, the particular values of the prescribed temperature at the top of the column become irrelevant and the reference value of ~ 7000 years, previously estimated for an idealised infinite domain, is retrieved. More generally, we prove that solutions with different upper boundary conditions, ~~yet~~ covered by our formulation, converge to the same result in such a limit. These results ultimately ~~manifest~~ illustrate a subtle connection between internal free (the binge-purge hypothesis) and externally-driven (~~in the sense of~~ a time-dependent boundary condition at the top) mechanisms caused by the finitude of the domain. ~~Thermomechanical instabilities , inherent to~~ Since thermomechanical instabilities (i.e., the transition between two plausible modes of basal lubrication governed by the thermal state of the ice) are the triggering mechanism of a binge-purge oscillator, internal free oscillations ~~, are in fact~~ are sensitive to the particular climatic forcing imposed as a boundary condition at the top of the ice column. Lastly, analytical solutions ~~herein presented~~ presented herein are applicable in any context where our ~~general~~ Robin boundary problem is satisfied.

Copyright statement. TEXT

1 Introduction

Periodic episodes of extreme iceberg discharge have captivated the glaciological and paleoclimatological community for the last three decades. Yet the ultimate cause of these so-called Heinrich Events (HE) remains elusive. Several mechanisms have been proposed in the literature that can be broadly classified into two branches: internal free and externally-driven oscillations.

Free oscillations were first proposed in MacAyeal (1993a) as manifestations of the Laurentide Ice Sheet (LIS) purging excess ice volume. This interpretation rests on the assumption that a transition exists between two potential states of basal lubrication (Alley and Whillans, 1991; Hughes, 1992) and it is known as the binge-purge hypothesis. Namely, when the basal ice temperature is below the pressure melting point, the ice sheet is assumed to be stagnant and it simply thickens due to snow accumulation. As a result of the geothermal heat flow, the ice column is expected to warm and the base eventually yields melting. At this point, the ice sheet is no longer at rest and begins to slide over a lubricated sediment bed. The purge phase continuous until the basal temperature gradient exceeds the value that can be maintained by the geothermal heat flux and the frictional energy dissipation combined. MacAyeal (1993a) thus investigated what causes the bed of the LIS in Hudson Bay and Hudson Strait to shift from a frozen to a thawed state as well as the time length involved in this process. To this end, he developed a conceptual model that shows how amplitude and periodicity depend on two environmental factors: the annual average sea-level temperature and the atmospheric lapse rate (MacAyeal, 1993a). Furthermore, a periodicity of $T \approx 7000$ years was estimated from these two factors for a simplified geometry. This value was determined as the time required for the base of a semi-infinite one-dimensional motionless ice column to reach the melting point due to a constant geothermal heat flow (analytically from Carslaw and Jaeger, 1988) and it marks the onset of the purge phase on a binge-purge cycle. The absence of time dependent boundary conditions throughout the study is noteworthy.

Even though both the period and amplitude of the free oscillations appear to be dependent on environmental factors, the same study dismissed the possibility of an oscillation period imposed by an external harmonic atmospheric forcing as a result of the strong amplitude attenuation with depth. In other words, if such a periodic external climate forcing did exist, its imprint would be negligible at the base of the ice sheet. To prove so, MacAyeal (1993a) showed that the corresponding e-folding decay length of a $T \approx 7000$ years periodicity reads $\sqrt{2k/\omega} = 314$ m for a motionless ice column. Moreover, a constant vertical velocity was also considered so as to account for a potential advection term, thus increasing the e-folding decay length to 970 m. In view of these results, it is evident that a harmonic surface temperature fluctuation would become negligible at the base of a thick ice sheet.

To provide quantitative support to the conceptual model, a low-order model of the HE cycle was additionally developed (MacAyeal, 1993b) to confirm that the theoretical estimation of HE periodicity T is in fact determined by the aforementioned environmental factors (MacAyeal, 1993a). In this two-dimensional model, ice flow mechanics and mass balance are combined in a manner that yields null horizontal ice flow when the base is frozen whereas deforming sediments allow for rapid sliding when the base is melted. Internal ice deformation is disregarded and ice thickness is assumed to be uniform along the cross section of the LIS (from Hudson Bay to the mouth of Hudson Strait). Remarkably, the numerical

periodicity showed a discrepancy from the theoretical estimation of solely 4%. However, this relaxation oscillator model assumes a characteristic ice stream purge timescale of 250 years, given the absence of explicit simulations of a Hudson Strait ice stream. Notably, this choice is relevant for the long timescale of the HE since it determines the switch from purge to growth behaviour, found to be 450 years in the numerical results.

Since then, dynamic 3D ice-sheet models have been used to investigate the mechanisms underlying HEs. For instance, Marshall and Clarke (1997) used a 3D model to simulate the LIS, though no discharges were reproduced within the wide range of model parameters. Calov et al. (2002) first modeled oscillatory behaviour in three-dimensional ~~SIA~~ Shallow Ice Approximation (SIA) models with *ad hoc* basal sliding. Along with other studies, the authors noted the necessary evolving drainage and till mechanics providing potential insight into our understanding of the physical processes that ~~causes~~ caused Hudson Strait oscillations (Calov et al., 2002; 2010). ~~Thus, from~~ From highly reduced models (e.g., Tulaczyk et al., 2000b) to a complex Herterich-Blatter-Pattyn ice model (e.g., Bougamont et al., 2011), multiple approaches have been found for a wide degree of comprehensiveness in ice stream dynamics in which the basal hydrology has become essential for an appropriate representation of the ice streams.

More recently, Robel et al. (2013) focused on the temporal variability of an ice stream accounting for basal hydrology, modeled as a ~~unique~~ single lumped spatial element assuming a single velocity to represent ice discharge. The surface temperature and the geothermal heat flux were found to ~~determine~~ be important controls of the character of the ice flow. In particular, an oscillatory binge-purge mode was also present and appeared to be primarily caused by re-freezing of meltwater due to ice thinning during stagnation. The remarkable dependence of both the periodicity and the amplitude of these events on the boundary conditions of the system (surface temperature and geothermal heat flux) suggests that even a zero-dimensional spatial model (i.e., a single spatial element) is highly sensitive to time-independent forcing.

Nevertheless, none of these studies discussed the theoretical implications of ~~a HE periodicity estimated~~ estimating HE periodicity under the assumption of a (oversimplified) ~~semi-inifinite~~ semi-infinite domain. In addition, these assumptions lack a more general treatment of the plausible boundary conditions at the top of the ice column. Despite the fact that the characteristic binge timescale determined the HE periodicity solely from environmental factors (lapse rate and sea level temperature) in prior studies, it does not necessarily imply that such periodicity is independent of the ~~boundary conditions~~ atmospheric temperature conditions and the energy balance across the ice-air interface. Strictly speaking, one can only conclude that the periodicity T cannot be imposed by ~~harmonic forcing~~ a harmonic forcing at the ice surface.

Even so, the $T \approx 7000$ year periodicity appears widely used in the literature as a reference value for ice-sheet models. Yet the theoretical implications of treating the problem with a more realistic finite medium remain unexplored. We herein investigate the consequences of considering a one-dimensional motionless ice column with a finite thickness L and quantify the impact of explicit boundary and initial conditions. A formulation of the problem is given in Section 2; the approach followed in this work is presented in Section 3; analytical solutions are shown in Section 4; results are discussed in ~~Section~~ Sections 5 ~~and~~, 6 and 7; our concluding remarks are given in Section ~~6.~~ 8.
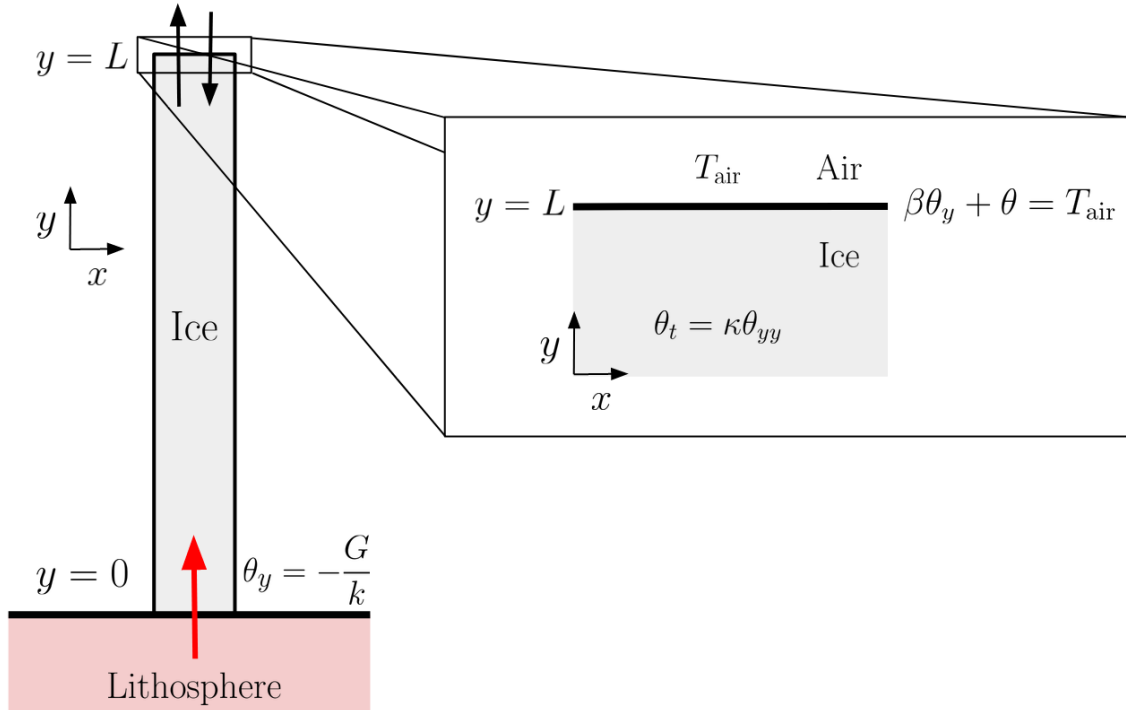
Figure 1. Schematic view of the motionless one-dimensional ice column with a finite thickness L. Temperature evolution is dictated by the heat equation and an appropriate set of initial and boundary conditions. Subscripts denote partial differentiation. At the top, both the ice temperature and the vertical gradient can vary in time, thus allowing for non-equilibrium thermal states across the ice-air interface. At the base, the vertical gradient is fixed to the value given by the geothermal heat flux $\theta_y = -G/k$. Note that our formulation is one-dimensional so that the x-axis is solely introduced for visualization.

2 Finite thickness

Let us now elaborate on the description of a more realistic one-dimensional ice column with a finite thickness L. Our domain is then defined as the interval $y \in [0, L] \equiv \mathcal{L}$. First, we must reformulate the problem imposing the necessary additional boundary condition at the top of the motionless column $y = L$ (Fig. 1).

In the simplest physical scenario, the ice surface temperature is set to the air temperature value $\theta(L, t) = T_{\text{air}}$. However, the particular surface temperature is in fact the result of the energy balance between the ice and the atmosphere. ~~The most~~ A more general approach considers that the ice and the air may not be always at thermal equilibrium, thus yielding a heat flux due to a vertical temperature gradient. The thermal equilibrium is only reached if the ice surface and the atmosphere temperatures are identical. In such conditions, the heat flux across the interface is null and the vertical gradient at the top the ice column vanishes. ~~As a result~~In this description, both the surface ice temperature and the vertical gradient can consequently vary in time:

$$\beta\theta_y + \theta = T_{\mathrm{air}}, \qquad y = L, \, t > 0, \tag{1}$$

100 where italic subscripts denote partial differentiation and β is a parameter with length dimensions ~~and italic subscripts denote partial differentiation.~~

~~The β factor~~ that modulates the permissible deviation between ice and air temperatures. Equation 1 falls within the so-called linear heat transfer boundary conditions (e.g., Carslaw and Jaeger, 1988, Chapter § 1.9) and β is often referred to as the surface thermal resistance (per unit area).

105 We can then physically interpret this parameter β as the thermal insulation of the ice-air interface. In other words, β is a length-scale over which the ice column feels the air temperature. A zero value corresponds to an ideal conductor ($\theta(L,t) = T_{\mathrm{air}}$), whereas $\beta \to \infty$ represents a perfect thermal insulator characterized by a null heat exchange across the interface. In the limit case $\beta = 0$, the interface ice-air is always at thermal equilibrium (i.e., $\theta = T_{\mathrm{air}}$). For $\beta \neq 0$, we allow for a heat exchange across the ice surface driven by the temperature difference between the two media. ~~The ice surface will consequently evolve in time~~
110 ~~towards T_{air}.~~

~~Thus~~Considering diffusive heat transport, the ice temperature $\theta(y,t)$ satisfies ~~the following~~ an initial value problem given by the heat equation:

$$\begin{cases} \theta_t = \kappa\theta_{yy}, & y \in \mathcal{L}, \, t > 0, \\ \theta = \theta_0(y), & y \in \mathcal{L}, \, t = 0, \\ \theta_y = -G/k, & y = 0, \, t > 0, \\ \beta\theta_y + \theta = T_{\mathrm{air}}, & y = L, \, t > 0, \end{cases} \tag{2}$$

where ~~the ice diffusivity is denoted by κ,~~ G is the geothermal heat flux~~and~~, k is the ice conductivity ~~.~~ and κ is the ice diffusivity
115 (assumed to be constant since we do not explicitly consider the firn layer above the ice).

The initial temperature profile reads $\theta_0(y) = \theta_{\mathrm{b}} + (\theta_{\mathrm{L}} - \theta_{\mathrm{b}})\,y/L$, where θ_{L} and θ_{b} are the initial ~~temperature~~ temperatures at the top and the base of the column~~respectively.~~, respectively. This linear profile is introduced for simplicity and it allows us to explicitly determine the impact of the initial basal/surface ice temperature independently.

We must stress that the system described as above (Eq. 2) builds upon MacAyeal (1993a) and aims at a purely vertical
120 diffusive heat-transfer description of a motionless ice column. In reality, heat transfer is well-known to be a three-dimensional process with a higher level of complexity that encompasses several mechanisms as horizontal/vertical advection, potential presence of liquid water within the ice, a varying ice thickness, internal heat deformation and frictional heat production among others. The current problem is approached by using analytical techniques and so the complexity of the system is critical if an analytical solution is to be found. The simplicity of our description provides new insight from a theoretical perspective.

3 Fourier method

Our aim is to solve the initial boundary value problem by using the Fourier method, also known as separation of variables (an overview of the method is given in Appendix A, for a standard reference see e.g., Kalnins et al., 2018). Consequently, we first need to find a change of variable that leaves us with homogeneous boundary conditions ~~(e.g., 'shifting the data' technique)~~ in order to determine the corresponding eigenvalues.

Let us then define the new variable $\xi(y, t)$ for the problem determined by ~~the equation Set~~ Eq. 2:

$$\xi = \theta - T_{\text{air}} + (y - \beta - L)\frac{G}{k} \tag{3}$$

Therefore, in terms of the new variable the problem under consideration reads:

$$
\begin{cases}
\xi_t = \kappa \xi_{yy}, & y \in \mathcal{L},\ t > 0, \\
\xi = f(y), & y \in \mathcal{L},\ t = 0, \\
\xi_y = 0, & y = 0,\ t > 0, \\
\beta \xi_y + \xi = 0, & y = L,\ t > 0,
\end{cases}
\tag{4}
$$

where the initial state is $f(y) = \theta_0(y) - T_{\text{air}} + (y - \beta - L)\frac{G}{k}$.

As a result, we now have a homogeneous problem that can be solved by separation of variables (Appendix A). If a solution exists, it determines the vertical temperature profile at any given time for the initial and boundary conditions provided by ~~the Set~~ Eq. 2.

4 Analytical solution

The solution $\xi(y, t)$ to the boundary problem determined by the Set 2 (derivation details in Appendix B) reads:

$$\xi(y, t) = \sum_{n=0}^{\infty} A_n \cos\left(\sqrt{\lambda_n}\, y\right) e^{-\kappa \lambda_n t}, \tag{5}$$

where the eigenvalues ~~$\sqrt{\lambda_n}$~~ λ_n are given by the transcendental equation:

$$\operatorname{\sout{tan}cot}\left(L\sqrt{\lambda_n}\right) = \frac{1}{\beta\sqrt{\lambda_n}} \beta\sqrt{\lambda_n}. \tag{6}$$

Equation 6 does not admit an algebraic representation, hence requiring a numerical method to compute λ_n. Here we implemented the Brent-Dekker algorithm (Dekker, 1969; Brent, 1971) with a tolerance of 10^{-8}. This root-finding algorithm choice combines the bisection method, the secant method and the inverse quadratic interpolation.

The coefficients A_n can be readily obtained applying orthogonality among eigenfunctions:

$$A_n = \frac{2}{L} \int\limits_0^L \xi(y,0) \cos\left(\sqrt{\lambda_n}y\right) dy. \tag{7}$$

It is noteworthy that if β is strictly zero (i.e., the ice surface temperature is prescribed $\theta(L,t) = T_{\text{air}}$), the ~~solution is still given by Eq. 5 but Eq. 6 no longer holds (see Appendix C). Rather, the eigenvalues satisfy~~ solution is equivalent to finding the eigenvalues satisfying the equation $\cos\left(L\sqrt{\lambda_n}\right) = 0$ and can be obtained analytically as:

$$\sqrt{\lambda_n} = \left(n + \frac{1}{2}\right)\frac{\pi}{L}, \tag{8}$$

where $n = 0, 1, 2, ...$

In this particular case, the corresponding coefficients A_n also allow for analytical expression:

$$A_n = 4(\theta_{\text{b}} - \theta_{\text{L}})\left[\frac{\cos(n\pi)}{2n\pi + \pi}\right] - 8L\frac{\tilde{G}}{k}\left[\frac{1}{2n\pi + \pi}\right]^2. \tag{9}$$

Table 1. Employed parameter values and range further explored in Fig 6.

Magnitude	Symbol (units)	Fixed value	MacAyeal (1993)	Explored range (Fig. 6)
Initial ice basal temperature	θ_{b} $(°C)$	-10.0	-10.0	[-50,-10]
Initial ice surface temperature	θ_{L} $(°C)$	-25.0	N/A	[-50,-10]
Geothermal heat flux	G (mW/m^2)	50.0	32.0	[25,100]
Air temperature	T_{air} $(°C)$	-25.0	N/A	[-50,-10]

5   Vertical temperature profile

We now present the vertical profiles $\theta(y,t)$ from analytical solutions given by Eq. 5 for three different thicknesses, $L = 1.0$, 1.5 and 2.5 km, at $t = 0$ and ~~$t = 4960$~~ $t = 4750$ years (Fig. 2) using the set of paramters described in Table 1. The second time frame value is chosen so that the fastest warming scenario (blue line in Fig. 2) precisely reaches melting.

~~Vertical profiles from analytical solutions $\theta(y,t)$ for three different ice-column thicknesses $L = 1.0$, 1.5, and 2.5 km. Top panel (a), $t = 0$ yr; bottom (b), $t = 4960$ yr. Solid line represents solutions for $\beta = 50$ m whereas the case $\beta = 0$ is denoted by a dotted line.~~ Since solutions are presented as infinite series, truncation was naturally required. We kept 100 terms in Eq. 5, though the error is below 0.03% after the 13th term.

The implications of a finite domain are ~~clear. The lower half of the column~~ quite notable. Particularly, the column base warms due to the geothermal heat flux ~~and this rate is in fact proportional to $\sim \kappa\lambda_n e^{-\kappa\lambda_n t}$~~ at a rate that is proportional to

(a) Initial temperature profile.

(b) Temperature profile after 4750 years.
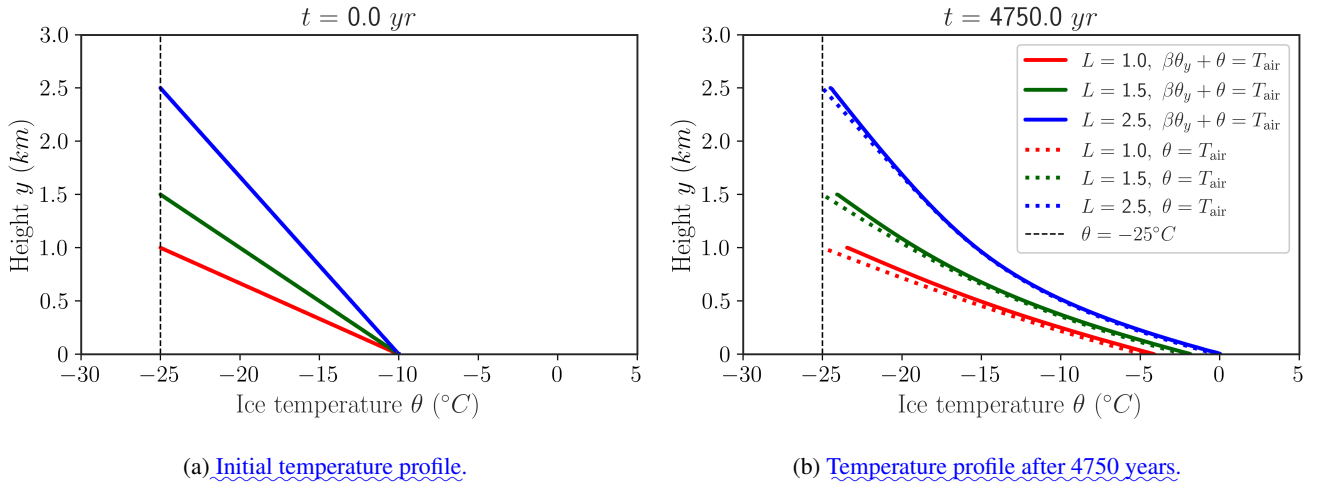
Figure 2. Vertical profiles from analytical solutions $\theta(y,t)$ for three different ice-column thicknesses $L = 1.0, 1.5$, and 2.5 km. Left panel (a), $t = 0$ yr; right (b), $t = 4750$ yr. Solid line represents solutions for $\beta = 100$ m where the case $\beta = 0$ is denoted by a dotted line. Parameter values employed are shown in Table 1 (fixed value column)

165   $\sim \kappa\lambda_0 e^{-\kappa\lambda_0 t}$ at leading order. Then if we let $\cancel{L_1 > L_2}$ $L > \tilde{L}$ be two thicknesses, it consequently yields $\cancel{|\partial\theta_1/\partial t| > |\partial\theta_2/\partial t|}$ that the ratio $\theta_t/\tilde{\theta}_t \sim e^{-\kappa(\lambda_0 - \tilde{\lambda}_0)t}$ exponentially grows, so that rate of change (at $y = 0$) is larger for a thicker column since the corresponding eigenvalues $\lambda_0 < \tilde{\lambda}_0$. That is, a thicker ice column implies a faster change of its basal temperature.

The impact of β is particularly clear at the top (Fig. 2b), where the temperature slightly increases due to an upward heat flux originating at the base (unlike the $\beta = 0$ case, where the temperature is prescribed). ~~The specific non-zero β value does~~

170   ~~not alter this behaviour, though larger values yield a greater temperature difference between the ice and the atmosphere.~~ We have chosen $\cancel{\beta = 50}$ $\beta = 100$ m to display such mechanism, whilst keeping a reasonable temperature difference (Cuffey and Paterson, 2010). ~~We can then physically interpret this parameter as the thermal insulation of the ice-air interface. Thus, a zero value corresponds to an ideal conductor ($\theta(L,t) = T_{\mathrm{air}}$), whereas $\beta \to \infty$ represents a perfect thermal insulator characterized by a null heat exchange across the interface~~

175   Figure 3 further focuses on the basal temperature evolution by comparing the effects of a particular zero/non-zero β value for different ice thicknesses, yet it does not provide information about the relevance of the particular β choice. The implications of this choice and their relative magnitude compared to the total thickness is thoroughly presented in Figs. 4 and 5. Since this thermal insulator parameter has length dimensions, it is illustrative to study its dependency referred to the particular column thickness L, i.e., the dimensionless quantity β/L shown in Fig. 4. As β becomes small compared to the ice thickness (i.e.,

180   $\beta/L \ll 1$), the ice surface remains cold by the influence of the atmosphere temperature ($T_{\mathrm{air}} = -25$ °C). The entire profile is affected by the surface condition and thus the basal temperature remains lower as well. On the contrary, if we let $\beta/L = \mathcal{O}(1)$, we find that the ice surface monotonically warms (due to the upwards geothermal heat flux and the imposed larger insulating
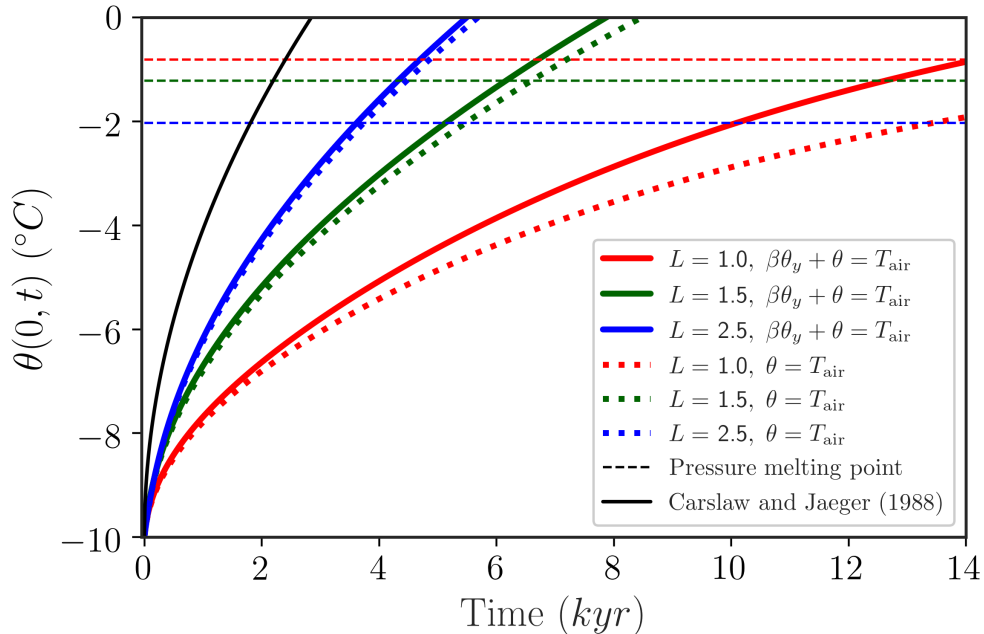
Figure 3. Time evolution of the basal temperature for three different thicknesses (in km). Solid line represents solutions for $\beta = 100$ m whereas the limit case $\beta = 0$ (i.e., fixed surface temperature) is denoted by a dotted line. The boundary condition at the base is identical for all cases and given by the geothermal heat flux G. The horizontal dashed lines represent the corrected pressure melting point for each column thickness.

condition) and the base reaches melting faster. This behaviour yields two points worth noting: (1) the saturation in basal temperature for $\beta/L > 0.5$ and (2) a "never-thawing" base for sufficiently low β/L values.

185   To complete our study on the impact of the particular β/L choice, we represent the ice surface temperature deviation from the air temperature boundary condition normalised by the latter as $\Delta\theta = (\theta(L) - T_{\text{air}})/T_{\text{air}}$ (blue solid line, Fig. 5). We thus obtain a dimensionless quantity that reflects the surface temperature changes as a function of the relative thermal insulation referred to the column thickness. The particular ice surface temperature is evaluated when the base reaches melting (red solid line, Fig. 5) so as to ensure that the incoming energy is entirely diffused and there are no phase changes. We find ice temperature 190   deviations up to a 30% from the air temperature (imposed as a boundary condition) in the limit $\beta/L \rightarrow 1$.

6   A new period for the binge/purge oscillator

~~First, we present the~~ Prior to a detailed discussion of our results, we must note that the solution to our Robin boundary problem (Eqs. 5 - 7) describes the evolution of the temperature profile only until the ice column base thaws, and therefore does not
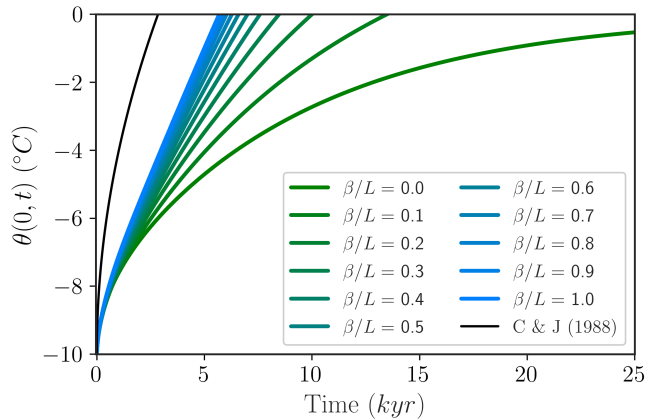
(a) ~~Time evolution of the basal temperature for three different thicknesses. Solid line represents solutions for $\beta = 50$ m whereas the limit case $\beta = 0$ (i.e., fixed surface~~ Basal temperature~~) is denoted by a dotted line. The boundary condition at the base is identical for all cases and given by the geothermal heat flux G.~~
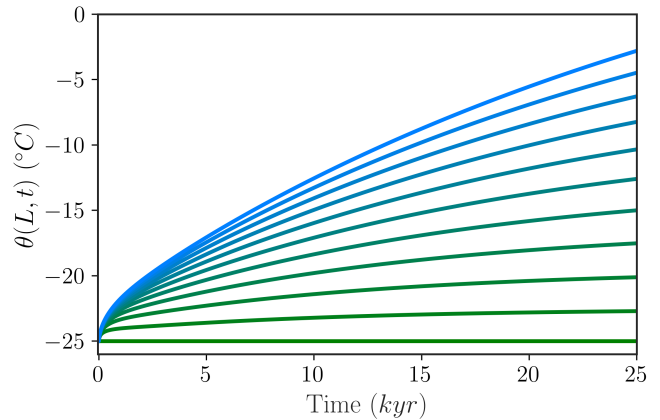
(b) Surface temperature.

Figure 4. Ice temperature time series for (a) Base and (b) Surface. Each line represents a particular dimensionless β/L choice. The strictly zero case corresponds to $\beta = 0$ and $L = 1.0$ km. A solid black lines denotes the semi-inifinite domain solution (Carslaw and Jaeger, 1988). The air temperature is fixed for all cases and reads $T_{\text{air}} = -25$ °C.

show a periodic behaviour of the ice dynamics. Such behaviour emerges once this solution is considered within MacAyeal's
195   oscillator (MacAyeal, 1993a, b).

The temporal dependency of the basal temperature (Fig. 3) from our analytical solution (Eq. 5) ~~. We further~~ allows us to calculate the time required for the column base to reach the melting point analogously to the growth phase of a Heinrich event oscillation (MacAyeal, 1993a)~~, hereinafter referred as potential periodicity~~ (Fig. 6. We also account for the pressure correction of the ice melting point as $\theta = \tilde{\theta} + \alpha P$, where $\alpha = 9.8 \cdot 10^{-8}$ K/Pa (e.g., Greve and Blatter, 2009). Knowing that $P = \rho g L$ and
200   our column spans the following thickness interval $L = [1.0, 3.5]$. For $\Delta L \simeq 3.0$ km, then $\tilde{\theta} \simeq -2.6$ ºC yields a non-negligible correction, making the ice thickness dependence even stronger as a result of two independent contributions: a more significant insulating effect of a thicker ice column and a larger pressure melting correction. It is worth stressing that the period of the binge-purge oscillator (MacAyeal, 1993a) did not considered any pressure melting correction so that a one-to-one comparison must dismiss such effect (see Section 7).

205   Figure 3 shows the sensitivity of the thermal state of the base to the thickness of the column L and to the ~~mathematical~~ treatment of the surface boundary condition. It is clear that the column thickness is ~~the primary~~ a fundamental factor that allows the surface temperature to influence the evolution of the base. Strictly speaking, the external forcing perturbs the temperature vertical profile of the ice column, thus determining the basal temperature. When we allow for non-equilibrium thermal states
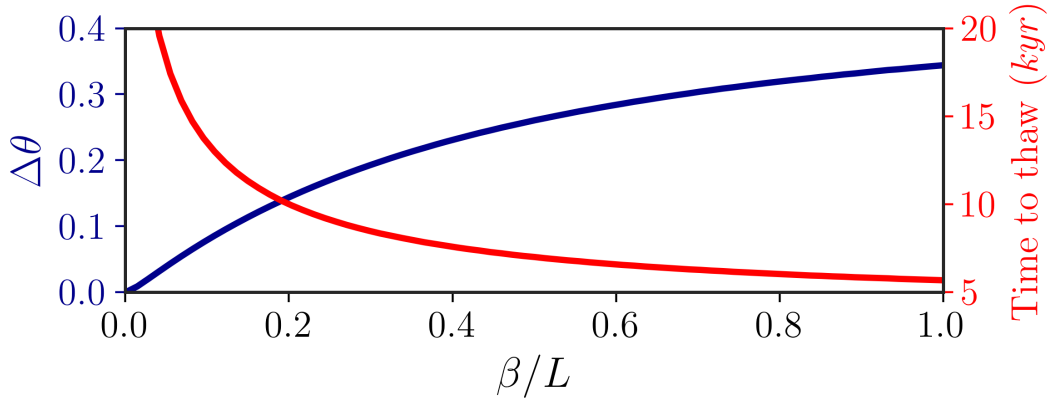
Figure 5. Normalised ice surface temperature deviation $\Delta\theta$ (dark blue line) from the air temperature boundary condition T_{air} and time required for the base to thaw (red line) as a function of the normalised insulating parameter β/L. The ice surface temperature deviation is evaluated when the base reaches melting.

in the top boundary condition (i.e., $\beta \neq 0$), the base warms faster since the column surface can evolve in time towards higher temperatures, thus inducing a lower temperature difference between the base and the top. The relevance of ~~such effect is quantified by~~ this effect is inversely proportional to the column thickness, becoming negligible for large L values.

~~For a fixed β and a particular initial state, the rate of change of the basal temperature solely depends on the column thickness L, the choice of G and T_{air}. Nevertheless, when~~ When computing the time required for the base to thaw, the initial temperature profile plays an essential role. The linear profile is imposed as the initial condition of our analytical solution (Eq. 5) and then, a broad range of θ_b and θ_L values is explored to quantify their impact on this timescale (Fig. 6). Ideally, the initial condition should be set by the temperature profile immediately after an event in the binge-purge cycle, yet such a profile is not available. A linear profile assumes that the temperature in the ice reflects a linear lapse rate in the atmosphere as the ice thickness builds up over time.

Figure 6 also shows the dependency of ~~the potential periodicity on both the initial and~~ this basal-thawing timescale on the boundary conditions in our general formulation (Eq. 1). The impact of the external forcing is evident from Fig. 6b. As we would expect, lower T_{air} values yield longer ~~potential periods~~basal-thowing timescales, though solely for ice thicknesses below ~ 2 km. ~~Otherwise~~For thicker ice, the periodicity appears to be independent of the surface ice temperature. We therefore find that~~$L = 2$~~, for this parameter choice (Table 1), $L_{\mathrm{thr}} = 2$ km is a threshold value ~~,~~above which the ~~periodicity~~ time required to thaw is decoupled of the top boundary condition. A distinct parameter choice will alter this particular value, yet we expect this behaviour to remain present.

~~The potential periodicity~~ Such a threshold is a compelling result and deserves further elaboration. Since here we focus on the time required for the base to thaw, it is fundamental to consider the temperature gradient between the base and the top. The vertical temperature gradient must be supported by the geothermal heat flux. If the surface is too cold, the heat provided by G

may not be sufficient to support a large enough temperature difference (within the column) so that the base reaches the melting point. For a given choice of G, k and T_{air}, there exists a minimum ice thickness L_{min} that yields a temperature gradient that allows for the base to thaw. For thinner columns, the base always remains frozen. This further translates in a sudden increase in the basal-thawing timescale (Fig. 6b). Although the value of this threshold depends on the physical properties of the ice and the boundary conditions (i.e., k, G and T_{air}), the mechanism still holds irrespective of the particular parameter choice.

The time required for the base to thaw decreases as the geothermal heat flux increases. A similar behaviour is found with increasing L due to the thermal insulating effect of the ice column, particularly for low geothermal heat flux values. This is consistent with what we expected, as a higher geothermal heat flux provides a larger amount of heat (per unit time) to the ice column.

The initial conditions are also essential to quantify the time required for the ice base to thaw. We have considered a linear initial vertical profile $\theta_0(y) = \theta_{\mathrm{b}} + (\theta_{\mathrm{L}} - \theta_{\mathrm{b}})\, y/L$, so as to understand the explicit dependency of the initial surface temperature θ_{L} and the initial basal temperature θ_{b} independently (Figs. 6c and 6d). Namely, the impact of θ_{L} is determined by the column thickness, with a more acute dependence for low L values. This was expected as the vertical temperature gradient increases for a fixed temperature difference between base and top if the column thickness is reduced. A never-thawing base is plausible when such a vertical gradient surpasses the value given by the geothermal heat flux. Lastly, the ~~potential periodicity~~ time required to melt the base appears to be rather sensitive to the initial basal temperature, rapidly ~~saturating to~~ reaching values above 25 kyr for ~~$\theta_{\mathrm{b}} < -11°C$~~ $\theta_{\mathrm{b}} < -40°C$.

Figure 6d particularly shows a non-monotonic behaviour of the basal-thawing timescale with respect to the ice thickness. To understand this behaviour there are several factors that must be considered simultaneously. It is illustrative to look at the vertical profiles shown in Fig. 2. The fact that T is non-monotonic with L at $\theta_{\mathrm{b}} < -30°C$ is a consequence of two factors: the necessary energy budget to warm an ice column and the vertical temperature gradient. For a fixed temperature difference between the base and the top, the former increases with L, whereas the latter decreases with L.

For slight variations of the thickness δL around $L = 1.5$ km, while fixing the initial basal temperature to e.g., $\theta_{\mathrm{b}} = -30°C$, the time required to thaw the base increases regardless of the sign of δL. In other words, it takes longer to reach the melting point either for a thinner or a thicker column. This local minimum is a balance between the total energy necessary to heat the column and the fact that a thinner one implies a larger vertical gradient for a fixed temperature difference between the base and the top. If we consider the effect of these factors explicitly: first, a thinner column requires a smaller amount of energy to increase the temperature of the column; however, considering the second factor, a thinner column would yield a larger vertical temperature gradient (ultimately yielding a slowdown in the warming rate as the geothermal heat flux is fixed in the BC). The combination of both effects allows for the local minima found in Fig. 6d.

7   The limit $L \to \infty$

Compared to previous work, the analytical solutions presented herein account for an additional degree of freedom in terms of the domain definition: the ice column thickness L. Nonetheless, ~~this~~ these solutions should converge under certain conditions to
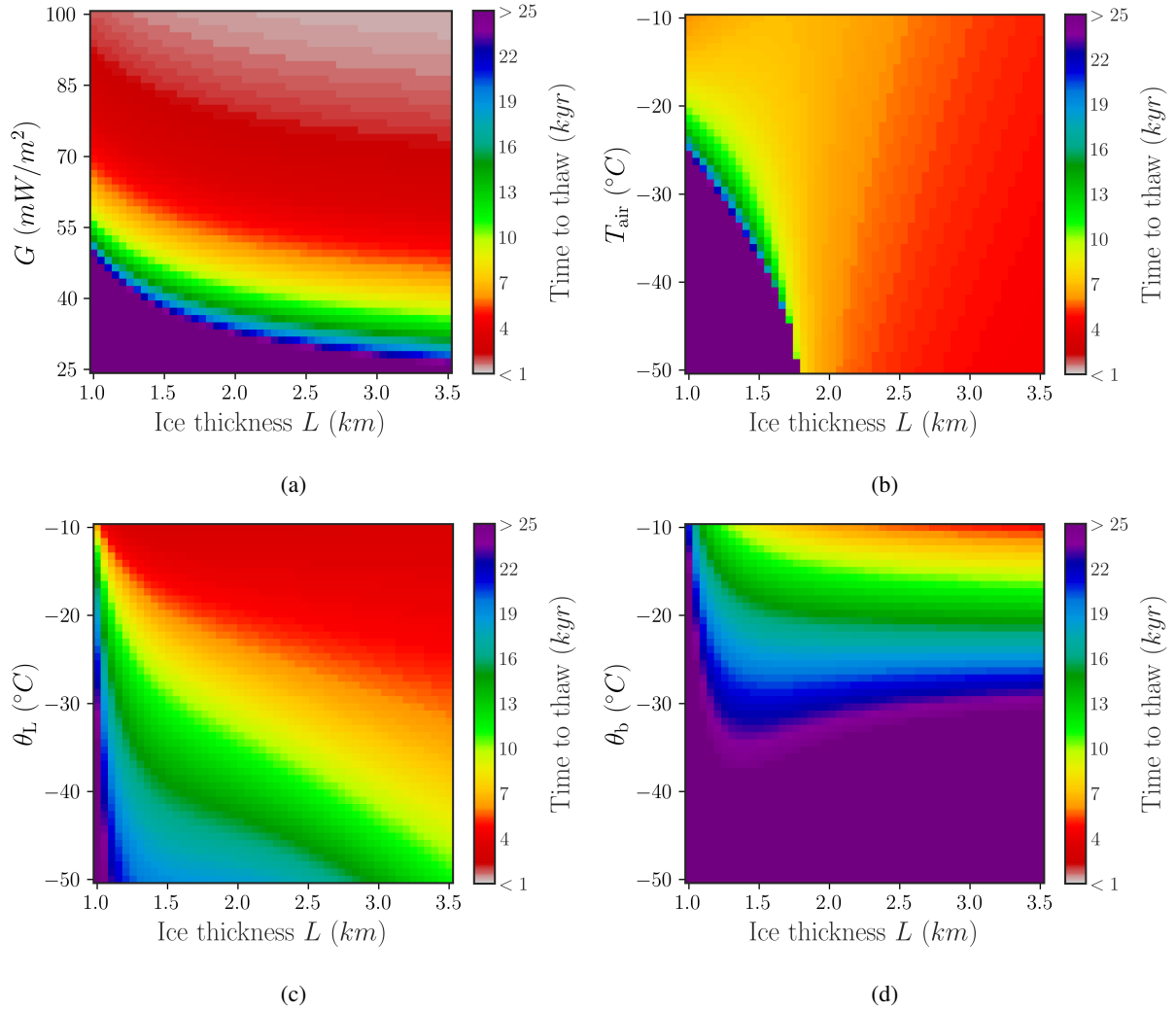
Figure 6. ~~Potential periodicity T~~ Time to reach the pressure melting point as a function of the ice thickness L, initial and boundary conditions in our general formulation. ~~$\beta = 50$~~ $\beta = 100$ m for all solutions. (Eq. 1). Boundary conditions: (a) Geothermal heat flux G and (b) Air temperature T_{air}. Initial conditions: (c) Initial ice surface temperature θ_L and (d) Initial basal temperature θ_b. Each panel represents the dependency of T to the explored range of values given in Table 1 while fixing the remaining variables.

the L-independent solution of Carslaw and Jaeger (1988) if we let $L \to \infty$. For completeness, we shall show that the theoretical periodicity of MacAyeal (1993a) is in fact retrieved in such limit irrespective of the specific boundary condition at the top.

The particular conditions under which our solution ~~converge~~ converges must imply an equivalent physical scenario to the one established by MacAyeal (1993a). Specifically, he considered an initial temperature profile that follows an atmospheric lapse rate Γ since the ice column is assumed to be assembled by snow precipitation. Hence the temperature solution is decomposed into a steady and a transient component, corresponding to Γ and the 'excess' of geothermal heat flux $\tilde{G} = G - k\Gamma$ respectively. In addition, pressure melting corrections were not considered. If we account for this particular formulation in our more general approach, the estimated 6944-year-period is retrieved in the limit $L \to \infty$ (Fig. 7).

Even though the eigenvalues of our problem satisfy a different relation in the limit $\beta = 0$, we shall prove that convergence to the 6944-year-period is independent of β and therefore consistent with previous results. Let φ and ϕ be two solutions of our general boundary problem (Set 2) with a zero and a non-zero β value respectively and arbitrary initial conditions. The difference between solutions is then:

$$\Delta \doteq \phi - \varphi = \sum_{n=0}^{\infty} \left[A_n \cos\left(\sqrt{\lambda_n} y\right) e^{-\kappa \lambda_n t} - \tilde{A}_n \cos\left(\sqrt{\tilde{\lambda}_n} y\right) e^{-\kappa \tilde{\lambda}_n t} \right]. \tag{10}$$

We must recall that the eigenvalues for a non-zero β case (i.e., ϕ) must satisfy Eq. 6. With an appropriate change of variable $x_n = L\sqrt{\lambda_n}$, it is clear that:

$$\lim_{L \to \infty} \left[\tan(x_n) = \frac{L}{\beta x_n} \right] \to x_n = \left(n + \frac{1}{2}\right)\pi, \tag{11}$$

~~where~~ since the right hand side goes to zero, we are thus left with roots of $\tan(x_n) = 0$. Note that $n = 0, 1, 2...$, which precisely correspond to the eigenvalues of the $\beta = 0$ case.

Hence, it is straightforward to see that the spatial and temporal dependency in Δ vanish in the limit $L \to \infty$. Additionally, given that the only L-order term is not proportional to β in the initial conditions, the coefficients A_n and $\tilde{A}_n$ become identical in such a limit. We then conclude that $\Delta = 0$ if β is finite as $L \to \infty$. In other words, we have proven that both solutions are ~~identical~~ asymptotically equivalent irrespective of β as the ice thickness approaches infinity.

MacAyeal (1993a) seemingly showed that the boundary conditions and the ice base temperature are decoupled by estimating that the e-fold decay of a periodic forcing with $\omega = 2.84 \times 10^{-11}\ s^{-1}$ in a motionless column reads $\sqrt{2k/\omega} = 314$ m. This estimation solely considers periodic signals, whilst leaving unexplored the implication of a non-periodic forcing. Our results affirm otherwise: though an oscillatory forcing rapidly attenuates with depth, Fig. 6 and 7 show that the base is in fact strongly coupled with both the external conditions and the initial thermal state of the ice. The strength of this coupling is determined by the column thickness L and the subsequent boundary conditions.

Figure 7 further shows that the ice thickness at which decoupling between the surface and the base occurs is almost independent of the top boundary conditions. In other words, we find that for MacAyeal (1993a)'s choice of geothermal heat flux $\tilde{G}$ (Table 1), the base evolves irrespective of the surface conditions for values $L > 3.0$ km.
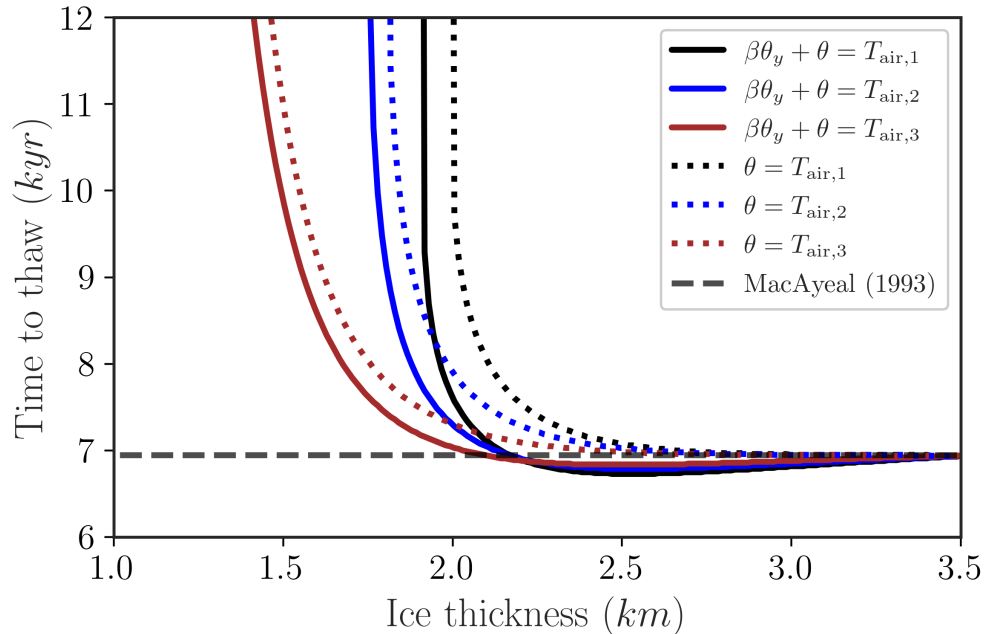
Figure 7. Time required for the column base to thaw as a function of the ice column thickness L, ~~allowing us~~ . This timescale is classically considered to ~~define~~ be the period of a binge-purge oscillator, a potential mechanism behind the Heinrich ~~Event periodicity from analytical solutions~~Events. ~~Colour represents~~ Colours represent the air temperature: $T_{\mathrm{air},1} = -40ºC$, $T_{\mathrm{air},2} = -30ºC$ and $T_{\mathrm{air},3} = -20ºC$. Solid line represents solutions for ~~$\beta = 50$~~ $\beta = 100$ m whereas the case $\beta = 0$ (i.e., fixed surface temperature) is denoted by a dotted line. The boundary condition at the base ~~$\theta_y = -\tilde{G}/k$~~ $\theta_y = -G/k$ is identical for all cases.

8 Conclusions

We have considered the implications of a finite one-dimensional ice column domain with a given thickness L on the solutions
295 of Fourier heat equation. The main purpose of the current work is to advance our understanding of how the thickness of an ice sheet influences its thermal evolution and further reconsider an important foundational piece of literature in the binge-purge hypothesis (MacAyeal, 1993a, b) in the more realistic setup of a finite thickness ice column and more general (Robin) boundary conditions. Unlike previous work, we provide analytical solutions that are explicitly dependent on this new degree of freedom L, thus quantifying its relevance without further approximations.

300 As a result of our new domain ~~extension~~definition, we have studied physically-plausible scenarios imposed by a ~~general~~ more general (Robin) boundary condition at the top of the motionless ice column. This approach considers that the ice and the air may not be always at thermal equilibrium, thus yielding a heat flux across the interface due to a vertical temperature gradient. As a result, both the ice temperature at the top and its vertical gradient are allowed to vary in time. If the ice surface happens to reach the air temperature, the vertical gradient vanishes leading to a thermal equilibrium state.

305   We find that the ice thickness plays a fundamental role in the Fourier solutions, which implies that a semi-infinite domain is an oversimplification (for the ice thickness range present in nature). The temperature at the base is highly dependent on the particular boundary condition at the top of the ice column. Particularly, these solutions are significantly distinct from each other for ice thicknesses $L < 2$ km.

    Our analytical approach allows us to quantify the sensitivity of the solution both to the initial and boundary conditions.
310 In ~~particular~~our particular parameter choice, the thermal state of the base completely decouples from the upper boundary condition (i.e., external forcing) for L values above 2 km and its thermal evolution becomes solely a function of the lower boundary condition (i.e., the geothermal heat flux). A distinct choice will alter this value, yet we expect this behaviour to remain present.

    Notably, in the limit $L \to \infty$, the prior L-independent solution (Carslaw and Jaeger, 1988) is retrieved, consequently yielding
315 the 6944 years periodicity estimated by MacAyeal (1993a). For completeness, we showed that such periodicity is in fact retrieved irrespective of the particular boundary condition at the top. This confirms the robustness of our results.

    Regarding a potential estimation of the binge-purge periodicity based on our analytical solutions, the new degree of freedom L entails strong consequences. First, large temporal variability can be explained solely by considering a change in ice thickness without any additional factors. In other words, this provides a source of natural internal variability irrespective of the external
320 forcing. For ~~medium-size~~ a 1-4 km thick ice sheets, this variability spans a 7-12 kyr range. In addition, the explicit consideration of distinct initial temperature profiles manifests a high sensitivity of the binge-purge oscillator period to its initial state.

    Moreover, a finite thickness also determines the mechanism by which an atmospheric perturbation might potentially influence the time required to melt the ice base since we have quantified the effect of a prescribed surface temperature and a vertical gradient. For a fixed L value, besides the geothermal heat flux, both the vertical gradient and the temperature at the top govern
325 the temperature time evolution, consequently defining the particular binge-purge periodicity estimation.

    It must be stressed that ~~,~~ even though we have shown that the ice base temperature is in fact coupled with the boundary conditions, the periodicity of ~~such events~~ the HE cannot be imposed by the frequency of an external forcing at the ice surface. Rather, the ~~potential period of the oscillator~~ timescale to reach melting conditions is determined by the ice thickness and the energy condition at the base and the surface.

330   Lastly, we note that a subtle connection exists between internal free (the binge-purge hypothesis) and externally-driven (in the sense of a time-dependent boundary condition at the top) mechanisms caused by the finitude of the domain. ~~Thermomechanical instabilities , inherent to~~ Since thermomechanical instabilities (i.e., the transition between two plausible stages of basal lubrication governed by the thermal state of the ice) are the triggering mechanism of a binge-purge oscillator, internal free oscillations ~~, are in fact~~ are sensitive to the particular climatic forcing imposed as a boundary condition at the top of the ice column. This double-
335 fold nature of thermomechanical instabilities is only exhibited when a finite domain is considered, further supporting the use of such analytical solutions in simple low-dimensional ice-sheet models where temperature profiles are otherwise prescribed.

Code availability. TEXT

Data availability. TEXT

Code and data availability. All scripts to obtain the results herein presented and to further plot figures can be found in: https://github.com/
340   d-morenop/Suplementary_ice-column-thermodynamics

Sample availability. TEXT

Video supplement. TEXT

Appendix A: Separation of variables

Let us briefly outline the separation of variables technique before elaborating on the solutions of our general problem. Consider
345   the following initial/boundary problem on an interval $\mathcal{I} \subset \mathbb{R}$,

$$
\begin{cases}
u_t = \kappa u_{yy} & y \in \mathcal{I}, t > 0 \\
u(y,0) = \varphi(y) & y \in \mathcal{I} \\
u \text{ satisfies certain BCs.}
\end{cases}
\tag{A.1}
$$

This technique looks for a solution of the form:

$$
u(y,t) = Y(y)T(t),
\tag{A.2}
$$

where the functions Y and T are to be determined. Assuming that there exists a solution of A.1 and plugging the function
350    $u = YT$ into the heat equation, it follows:

$$
\frac{T'}{\kappa T} = \frac{Y''}{Y} = -\lambda,
\tag{A.3}
$$

for some constant λ. Thus, the solution $u(y,t) = Y(y)T(t)$ of the heat equation must satisfy these equations. Additionally, in
order for u to satisfy the boundary conditions, we arrive to:

$$
\begin{cases}
Y''(y) = -\lambda Y(y) & y \in \mathcal{I} \\
Y \text{ satisfies our BCs.}
\end{cases}
\tag{A.4}
$$

This is a well-known eigenvalue problem. Namely, a constant λ that satisfies Eq. A.4 for some function X (not identically zero) is called an eigenvalue of $-\partial_y^2$ for the given boundary conditions. Hence, the function Y is an eigenfunction with associated eigenvalue λ.

Therefore, in order for a function of the form $u(y,t) = Y(y)T(t)$ to be a solution of the heat equation on the interval $\mathcal{I} \subset \mathbb{R}$, T must be a solution of the ODE $T' = -\kappa\lambda T$. Direct integration leads to:

$$T(t) = Ae^{-\kappa\lambda t}, \tag{A.5}$$

for an arbitrary constant A. Thus, for each eigenfunction Y_n with corresponding eigenvalue λ_n, we have a solution T_n such that:

$$u_n(y,t) = Y_n(y)T_n(t), \tag{A.6}$$

is a solution of the heat equation on our interval $\mathcal{I}$ which satisfies the BC. Moreover, given that the problem A.1 is linear, any finite linear combination of a sequence of solutions $\{u_n\}$ is also a solution. In fact, it can be shown that an infinite series of the form:

$$u(y,t) \equiv \sum_{n=1}^{\infty} u_n(y,t), \tag{A.7}$$

will also be a solution of the heat equation on the interval $\mathcal{I}$ that satisfies our BC, under proper convergence assumptions of this series. The discussion of this issue is beyond the scope of this work.

Appendix B: Solution of the problem

Let us elaborate on the solution of our general problem (Section 4) by first solving the associated eigenvalue problem. As we employ the separation of variables technique, the solution takes the form:

$$\xi(y,t) = \sum_{n=0}^{\infty} Y_n(y)T_n(t), \tag{B.1}$$

where the functions $Y_n(y)$ and $T_n(t)$ are to be determined. After the consequent change of variable so that $Y(y)$ satisfies Eq. A.4, we arrive to:

$$Y_n(y) = A_n\cos\left(\sqrt{\lambda_n}y\right) + B_n\sin\left(\sqrt{\lambda_n}y\right), \tag{B.2}$$

where A_n and B_n are to be determined. Applying the boundary conditions imposed in Set 2, it is clear that all sine coefficients are identically zero $B_n = 0$ and the eigenvalues $\sqrt{\lambda_n}$ are given by the transcendental equation:

$$\tan\cot\left(L\sqrt{\lambda_n}\right) = \frac{1}{\beta\sqrt{\lambda_n}}\beta\sqrt{\lambda_n}, \tag{B.3}$$

380 that admits no algebraic representation, hence requiring a numerical method to compute λ_n.

From orthogonality of the eigenfunctions $Y_n(y)$, the coefficients A_n of our solution are calculated following:

$$A_n = \frac{2}{L}\int_0^L \xi(y,0)\cos\left(\sqrt{\lambda_n}y\right)dy. \tag{B.4}$$

where $\xi(y,0) = \frac{\tilde{G}}{k}(y - L) - \theta_L + \theta_b$. Even though

Even though the eigenvalues of the problem are given by a trascendental equation with no algebraic representation, $\xi(y,0)$

385 is a function of the form $f(y) = ay + b,$ the integration of $f(y) = a + by$ and the coefficients A_n does not yield analytical representation since the eigenvalue equation is transcendental yield an explicit integration:

$$A_n = \frac{2}{L}\frac{\sqrt{\lambda_n}(a + bL)\sin\left(\sqrt{\lambda_n}L\right) + b\cos\left(\sqrt{\lambda_n}L\right) - b}{\lambda_n} \tag{B.5}$$

where $a = G/k + (\theta_L - \theta_{sl})$ and $b = \theta_{sl} - T_{air} - (\beta + L)G/k$.

Hence, the solution of our general problem reads:

$$\xi(y,t) = \sum_{n=0}^{\infty} A_n\cos\left(\sqrt{\lambda_n}y\right)e^{-\kappa\lambda_n t}, \tag{B.6}$$

Appendix C: Limit case $\beta = 0$

It is crucial to consider that the eigenvalue equation given by Eq. 6 does not hold for $\beta = 0$. In such case, after the consequent change of variable so that $Y(y)$ satisfies Eq. A.4, we arrive to:

$$Y_n(y) = A_n\cos\left(\sqrt{\lambda_n}y\right) + B_n\sin\left(\sqrt{\lambda_n}y\right), \tag{C.1}$$

395 where A_n and B_n are to be determined. Applying the boundary conditions imposed in Set 2, it is clear that all sine coefficients are identically zero, $B_n = 0$, and the eigenvalues read:

$$\sqrt{\lambda_n} = \left(n + \frac{1}{2}\right)\frac{\pi}{L}, \tag{C.2}$$

where $n = 0, 1, 2, \ldots$.

From orthogonality of the eigenfunctions $Y_n(y)$, the coefficients A_n of our solution are calculated following:

$$A_n = \frac{2}{L} \int_0^L \xi(y, 0) \cos\left(\sqrt{\lambda_n} y\right) dy. \tag{C.3}$$

where $\xi(y, 0) = \frac{\tilde{G}}{k}(y - L) - \theta_{\mathrm{L}} + \theta_{\mathrm{b}}$. Since $\xi(y, 0)$ is a function of the form $f(y) = ay + b$ and the eigenvalues allow for an analytical expression, the integration of the coefficients A_n is straightforward:

$$A_n = 4(\theta_{\mathrm{b}} - \theta_{\mathrm{L}}) \left[\frac{\cos(n\pi)}{2n\pi + \pi}\right] - 8L\frac{\tilde{G}}{k} \left[\frac{1}{2n\pi + \pi}\right]^2. \tag{C.4}$$

It is clear that this series converges and satisfies the initial condition imposed by $\xi(y, 0)$ given that:

$$\sum_{n=0}^{\infty} \frac{\cos(n\pi)}{2n\pi + \pi} = \frac{1}{4}, \tag{C.5a}$$

$$\sum_{n=0}^{\infty} \frac{1}{(2n\pi + \pi)^2} = \frac{1}{8}. \tag{C.5b}$$

Hence, the solution of Problem 1 reads:

$$\zeta(y, t) = \sum_{n=0}^{\infty} A_n \cos\left(\sqrt{\lambda_n} y\right) e^{-\kappa \lambda_n t}, \tag{C.6}$$

Author contributions. Daniel Moreno Parada formulated the problem, derived the analytical solutions, analysed the results and wrote the paper. All other authors contributed to analyse the results and writing the paper.

Competing interests. Alexander Robinson is an editor of The Cryosphere. The peer-review process was guided by an independent editor, and the authors have also no other competing interests to declare.

Disclaimer. TEXT

Acknowledgements. ~~Daniel Moreno, Alexander Robinson and Jorge Alvarez-Solas were~~ This research has been supported by the Spanish Ministry of Science and Innovation ~~project ICEAGE (~~(project IceAge, grant no. PID2019-110714RA-100)~~. Alexander Robinson was also~~

supported by , the Ramón y Cajal Programme of the Spanish Ministry for Science, Innovation and Universities (grant no. RYC-2016-20587) and the European Commission, H2020 Research Infrastructures (TiPES, grant no. 820970).

References

Alley, R. and Whillans, I.: Changes in the West Antarctic ice sheet, Science, 254, 959, 1991.

420 Bougamont, M., Price, S., Christoffersen, P., and Payne, A. J.: Dynamic patterns of ice stream flow in a 3-D higher-order ice sheet model with plastic bed and simplified hydrology, Journal of Geophysical Research, 116, https://doi.org/10.1029/2011jf002025, 2011.

Brent, R.: Brent, Richard P. An algorithm with guaranteed convergence for finding a zero of a function., The computer journal, 14, 422–425, 1971.

Calov, R., Ganopolski, A., Petoukhov, V., Claussen, M., and Greve, R.: Large-scale instabilities of the Laurentide ice sheet simulated in a

425 fully coupled climate-system model, Geophysical Research Letters, 29, 69–1, 2002.

Calov, R., Greve, R., Abe-Ouchi, A., Bueler, E., Huybrechts, P., Johnson, J. V., Pattyn, F., Pollard, D., Ritz, C., Saito, F., and Tarasov, L.: Results from the Ice-Sheet Model Intercomparison Project–Heinrich Event Intercomparison (ISMIP HEINO), Journal of Glaciology, 56, 371–383, https://doi.org/10.3189/002214310792447789, 2010.

Carslaw, H. S. and Jaeger, J. C.: Conduction of heat in solids, Clarendon Press, Oxford, 1988.

430 Cuffey, K. M. and Paterson, W. S. B.: The Physics of Glaciers, ACADEMIC PR INC, https://www.ebook.de/de/product/10550595/kurt_m_cuffey_w_s_b_paterson_the_physics_of_glaciers.html, 2010.

Dekker, T.: Finding a zero by means of successive linear interpolation., Constructive Aspects of the Fundamental Theorem of Algebra, B. Dejon and P. Henrici, Eds., Wiley Interscience, London, 1969.

Greve, R. and Blatter, H.: Dynamics of Ice Sheets and Glaciers, Springer Berlin Heidelberg, https://doi.org/10.1007/978-3-642-03415-2,

435 2009.

Hughes, T.: On the pulling power of ice streams, Journal of Glaciology, 38, 125–151, https://doi.org/10.3189/s0022143000009667, 1992.

Kalnins, E. G., Kress, J. M., and Jr, W. M.: Separation of Variables and Superintegrability The symmetry of solvable systems, IOP Publishing, https://doi.org/10.1088/978-0-7503-1314-8, 2018.

MacAyeal, D. R.: Binge/purge oscillations of the Laurentide ice sheet as a cause of the North Atlantic's Heinrich events, Paleoceanography,

440 8, 775–784, 1993a.

MacAyeal, D. R.: A low-order model of the Heinrich event cycle, Paleoceanography, 8, 767–773, 1993b.

Marshall, S. and Clarke, G.: A continuum mixture model of ice stream thermomechanics in the Laurentide Ice Sheet 2. Application to the Hudson Strait Ice Stream, Journal of Geophysical Research, 102, 20 615–20, 1997.

Robel, A. A., DeGiuli, E., Schoof, C., and Tziperman, E.: Dynamics of ice stream temporal variability: Modes, scales, and hysteresis, Journal

445 of Geophysical Research: Earth Surface, 118, 925–936, https://doi.org/10.1002/jgrf.20072, 2013.

Tulaczyk, S., Kamb, W. B., and Engelhardt, H. F.: Basal mechanics of Ice Stream B, west Antarctica: 2. Undrained plastic bed model, Journal of Geophysical Research: Solid Earth, 105, 483–494, https://doi.org/10.1029/1999jb900328, 2000b.